Kagome Lattice Hubbard model at half filled

Siegfried Guertler[1]

[1]Lehrstuhl für Theoretische Physik II, Technische Universität Dortmund, 44221 Dortmund, Germany

(Dated: February 27, 2014)

We investigate the Kagome lattice Hubbard model at half filled with respect to the Dirac, Uniform and dimerized state. It appears that even in the large-U limit the Dirac state being the optimal state in the Heisenberg model within VMC cannot be recovered as long as U stays finite. While the finite U allows the introduction of vacancies in a different manner compared to the $t-J$ model, the physics appears to have many similarities. We observe an impact of the dimerization on a possible Mott-transition in this model.

arXiv:1402.6612v1 [cond-mat.str-el] 26 Feb 2014

Introduction: The Kagome lattice is the prototype lattice to study effects of geometric frustration. Numerical methods such as variational Monte-Carlo (VMC), density matrix renormalization group (DMRG), exact diagornalization (ED) and series expansion (SE) have been used to clarify the ground state of the quantum Heisenberg model [1–6] on the Kagome lattice. Initially various Spin-liquid and Valence Bond Crystal/Solid states have been suggested, meanwhile there is strong indication for a spin-liquid state. The type of spin-liquid (including the questions whether it is a gapped or gapless spin liquid) state is still debated. Close in energy are different types of Valence Bond Crystal (VBC) states and the uniform spin-liquid state. Within variational Monte-Carlo the Dirac Spin Liquid (DSL) state appears best. Recently interest in the doped and diluted variants of the model arose. In part because of the situation in $ZnCu_3(OH)_6Cl_2$ as it is so far the best candidate of an structurally ideal Kagome lattice. This compound has very interesting experimental properties while impurities are present [7–12]. It consists of Kagome layers linked by Zn-Ions. In the Kagome plane Cupper Ions form the Kagome net and have an antiferromagnetic spin-1/2 interaction. Upon synethization of this compound some of the Zn-Ions exchange position with some of the Cu-Ions (around five percent of them).

An earlier work of one of us, found that doping the infinite U-case ("t-J" model) changes the state drastically from a the Dirac spin-liquid at half filled, to a valence bond crystal (VBC) [18, 19] for finite but small doping. Another interesting case is the Hubbard model at half-filled: Here the model is not doped, but as the U is tuned away from the infinite case, double occupation is possible. The Hubbard model on the Kagome has been investigated mostly with regard of a possible Mott-transitions [13–15] and for the special case of van-Hove filling [16, 17]. As indicated above actual compounds on the Kagome are mostly modeled with the Heisenberg model. The large but finite U is quite relevant for actual compounds too, as applying pressure would change the t/J ratio, implying that experimentally one may reach a Hubbard model through this route. On the other hand the study of the Hubbard model on the Kagome provides a nice playground to study the effects of frustration for both, charge and spin-degree of freedom.

The question we address in this paper is the physics of the half-filled Hubbard model, with special emphasis to the large U limit. Particularly we are interested if the large U Hubbard model is able to recover the Dirac spin-liquid state found in the Heisenberg model in the Mott phase of the half-filled Hubbard model. We ask the question whether the physics by tuning U differs or is similar to the case of introduction of vacancies by doping in the infinite U case [18, 19], particularly if a dimerized state forms. Our paper is a first step to understand the complicated and possible rich physics in the Kagome lattice Hubbard model. We find that while the physics appears qualitatively the same when tuning U compared to introducing vacancies by doping for the $t-J$ model, we are not able to recover the situation at the Heisenberg point. Below we discuss the likely reasons and implications of our findings.

Model and Method: As depicted in Fig. 1 the Kagome lattice consists of corner-sharing triangles, and has a physical unit-cell of 3 sites. We study the standard Hubbard model on the Kagome lattice defined as:

$$H = -t\sum_{\langle ij\rangle}\sum_{\sigma=\uparrow\downarrow}\left(c^{\dagger}_{i\sigma}c_{j\sigma}+\text{h.c.}\right)+U\sum_{i} n_{i\uparrow}\cdot n_{i\downarrow} \quad (1)$$

Here $c_{j\sigma}$ is the electron annihilation operator of an electron with spin σ on site i, $\vec{S}_i$ is the spin-1/2 operator at site i, and $n_{i\sigma}=c^{\dagger}_{i\sigma}c_{i\sigma}$. The sum $\langle i,j\rangle$ is over all the n.n. pairs. We set the n. n. hopping $t_{i,j}=t=1$ as the energy unit and the on-site repulsion U as tuning parameters. Within VMC the best state of the Heisenberg model is the Dirac spin-liquid state [20–22]. This state has a π-flux in the hexagon, and zero-flux in the triangles. Competitive is the uniform spin-liquid state and the valence bond crystal state, with the 12-site unit cell proposed by Hastings [20] (see Fig. 2 for the 3 states). Upon introducing doping in the large-U limit ($t-J$-model) the uniform spin-liquid state has a lower energy than the Dirac spin-liquid. Further the mentioned valence-bond-crystal is formed [18, 19]. Now we are introducing

holes not by removing electrons from half-filled, but by allowing double-occupation, when tuning U away from the large-U limit. Naturally we consider these 3 states in our investigation. In the Hubbard model there are two projectors which one should always consider in order to describe the physics and a possible Mott-transition correctly: the partial projection and the Holon-Doublon Binding factors. The partial projector is defined as:

$$\mathcal{P}_d = \prod_i (1 - \alpha n_{i\uparrow} n_{i\downarrow}) \tag{2}$$

where the product is over all lattice sites and projects out double occupied sites in dependence of the chosen variational parameter α with $\alpha = 1.0$ meaning a full projection with no double occupied states. We introduce the Holon-Doublon Binding factor, being necessary to accurately describe the intermediate coupling region:

$$\mathcal{P}_q = \prod_i (1 - \mu_q \mathcal{Q}_j) \tag{3}$$

$$\mathcal{Q}_j = d_j \prod_{\vec{r}} (1 - h_{j+\vec{r}}) + h_j \prod_{\vec{r}} (1 - d_{j+\vec{r}}) \tag{4}$$

with $d_j = n_{j\uparrow} n_{j\downarrow}$, $h_j = (1 - n_{j\uparrow})(1 - n_{j\downarrow}$ and μ_q a variational parameter between 0 and 1. This factor is necessary in the pure Hubbard model, as has been show in the past literature, without it only the low U limit will be captioned well and the wave-function would give considerable higher energy. Alternatively one can include a J-term with spin-spin exchange in the Hamiltonian, as the so called 'Hubbard-Heisenberg'-model [23]. These projectors are acting on our base wave-function as described above:

$$|\Psi_{\mathrm{VBC},\alpha}\rangle = \mathcal{P}_d |\Psi_{\mathrm{VBC}}\rangle \tag{5}$$
$$|\Psi_{\mathrm{Dirac},\alpha}\rangle = \mathcal{P}_d |\Psi_{\mathrm{Dirac}}\rangle \tag{6}$$
$$|\Psi_{\mathrm{Uniform},\alpha}\rangle = \mathcal{P}_d |\Psi_{\mathrm{Uniform}}\rangle \tag{7}$$

and finally:

$$|\Psi_{\mathrm{VBC},\alpha,q}\rangle = \mathcal{P}_q |\Psi_{\mathrm{VBC},\alpha}\rangle \tag{8}$$
$$|\Psi_{\mathrm{Dirac},\alpha,q}\rangle = \mathcal{P}_q |\Psi_{\mathrm{Dirac},\alpha}\rangle \tag{9}$$
$$|\Psi_{\mathrm{Uniform},\alpha,q}\rangle = \mathcal{P}_q |\Psi_{\mathrm{Uniform},\alpha}\rangle \tag{10}$$

We are using a standard VMC scheme with periodic boundary conditions. In the large-U limit the finite size effect is tiny starting from the $3 \times 8 \times 8$ lattice. We have investigated mainly sizes of 8×8 unit cells and compared with a few runs at larger 10×10 unit cells sizes, which showed little derivation. Note that due to several variational parameters and the larger Hilbert space of the Hubbard model compared to the $t - J$ and Heisenberg model, the computation of these sizes are indeed computationally challenging. We use 8-64 independent runs per data point (defined by a specific set of parameters) for which we thermalized for 20.000-80.000 sweeps and measured for up to 700.000 sweeps.

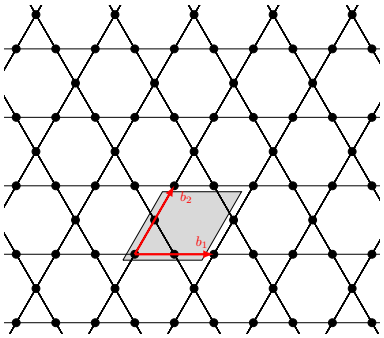

FIG. 1: (Color online) The Kagome lattice, consisting of corner-sharing triangles.

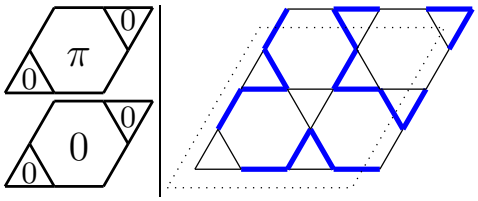

FIG. 2: (Color online) The variational states considered. Above left: Dirac state; Below left: Uniform state; Right: VBC state; the blue thick bonds corresponds to the VBC of Hastings and are controlled by χ_1.

Results: Let us first address the question whether the D-state is favorable in any regime for finite U: In Fig. 3 (a) we plotted the energy of the U- and the D-state as a function of U. We see that the D-state gradually comes closer in terms of energy to the best variational state, but it never has the lowest energy. This remains true in the large U limit as can be seen in the inset for a value of U up to 60. The binding-factor μ indicates the position of the Mott-transition (Fig. 3 (c)) which is at about $U \approx 11$ for the U-state and $U \approx 7$ for the D-state. We notice that both projectors α and μ rise quicker for the D-state. It appears that any introduction of vacancies and therefore mobility in the system renders the D-state as unfavorable. In Fig. 3 (b) we show the spin-spin exchange. After the Mott-transition this value saturates at a little below $S_i S_j \approx 40$ the large U limit gives a value of $S_i S_j \approx 40.5$.

Now we would like to focus on the question whether a dimerized state similar to the one found in the $t-J$ model is favorable. The U-state is contained in the HVBC-state, as they are equivalent when $\chi = 1.0$. We show all the relevant data in Fig. 4, which are the variational param-

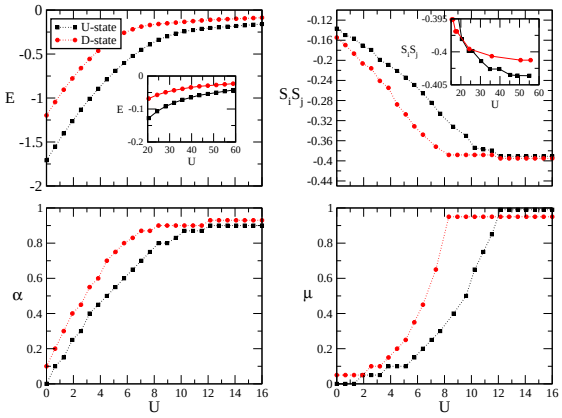

FIG. 3: (Color online) Comparison between the Uniform and Dirac state of energy E (a), spin-spin exchange S_iS_j (b), projection α (c) and binding factor μ (d). The Uniform state has always lower energy. System size: 8×8 unit cells.

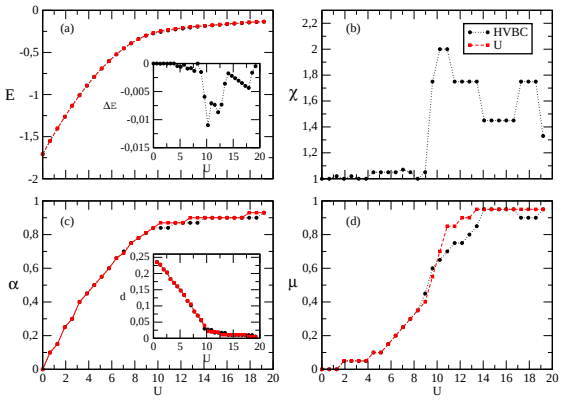

FIG. 4: (Color online) Comparison of the dimerized (HVBC) state with the uniform state (U-state). (a) Optimized energy and in the inset the energy difference between the U- and HVBC state, (b) Variational parameter χ, (c) projection parameter α and in the inset measured double occupancy and (d) holon-binding factor μ.

eters α, μ and χ, and the measured quantities energy E and double occupancy d. We compare the data for the case where we vary χ with the U-state where $\chi = 1.0$. In (a) of this Fig. we show the energies, which of course are close to each other, we plot the energy difference in the inset. Starting from $U \approx 9$ the dimerized state has a lower energy, the biggest gain for $U \approx 10$ where $\Delta E \approx 0.01$ (with a measured error-bar approx 0.002). While for all $U > 9$ we find an energy gain for $\chi > 1.0$ this gain is decreasing with larger U and cannot is within the error-bar for $U > 18$. Observing the evolution of χ with U we see a rather strong response of χ at $U = 9$. Note that we chose a fine spacing for χ for values close to 1.0 ($\Delta\chi \approx 0.01$) and a large spacing for the values close to 2.0 ($\Delta\chi \approx 0.2$) capturing the overall situation well, and being a more

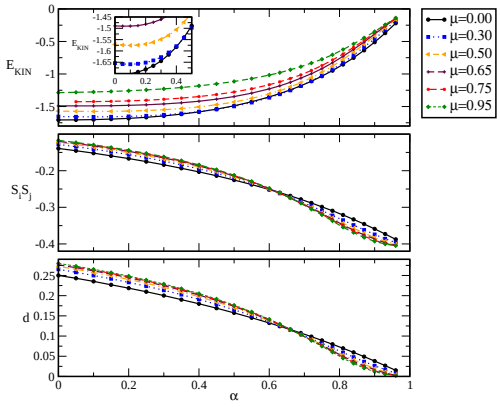

FIG. 5: (Color online) Impact of α on the energetics for given μ: kinetic energy $c_i^\dagger c_j$, spin-spin exchange S_iS_j and double occupation.

economic solution for computation. We see there is little difference in optimized value of α and the measured double occupation d when comparing the HVBC-state with the U-state. The doublon-holon binding however shows differences: For the uniform state we see a sharp rise, typically for a Mott-transition (similar to studies of the unfrustrated Hubbard model with the same method), for the HVBC-state on the other hand, μ takes longer to rise to the same value. This area is exactly the regime where the dimerized state has the highest energy gain.

In the $t-J$ model we observe the formation of this particular HVBC upon introducing holes by doping. In the Hubbard model we introduce holes by allowing double occupation. We see now that this other form of introduction of vacancies has a similar impact: Reduction of the value of U introduces more and more holes and similar to the case of the $t-J$ model the dimerization sets in, but is destroyed for a large amount of holes (here low U). It is clear that doping the Hubbard model would show a much stronger response to this instability, which is an aspect we leave for future investigation. Interesting is the interplay of the dimerization with the possible Mott-transition.

As argued in an earlier reference by us [19] the optimal doping level for the considered HVBC in the $t-J$ model is excepted to be at a doping of $\frac{1}{12} \approx 0.08333$, further the dimerized state is found between the doping of $\delta \approx 0.25$ to $\delta \approx 0.05$ [18]. In the Hubbard model at half-filled, holes are formed when other sites are double-occupied being controlled by the projection operation and the doublon holon-factor (see discussion below). We measure the effective double-occupation (Fig. 4 (c)) or vacant sites (which are in the half-filled case equivalent). We measure $\langle d \rangle = 0.025$ at the point with maximum dimerziation ($U = 10.8$) and $\langle d \rangle = 0.006$ at $U = 18$ where dimerization vanishes or becomes to tiny to measure. That means that we have fewer holes for dimerization compared to the

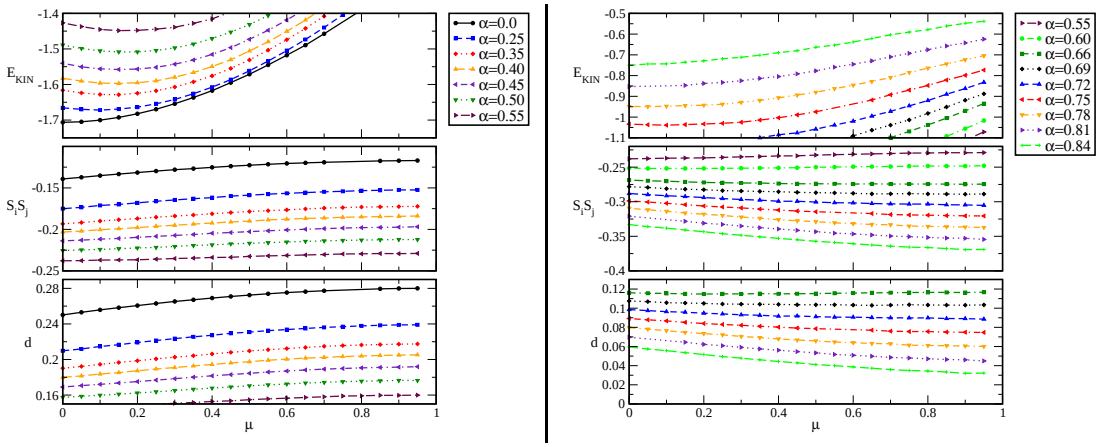

FIG. 6: (Color online) (left) Impact of μ on the energetics: kinetic energy $c_i^\dagger c_j$, spin-spin exchange S_iS_j and double occupation for low values of α (right) and high values of α.

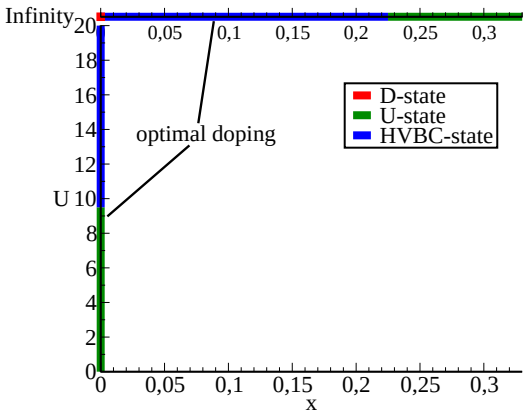

FIG. 7: (Color online) Phase-diagram combined with the results of two earlier references by us.

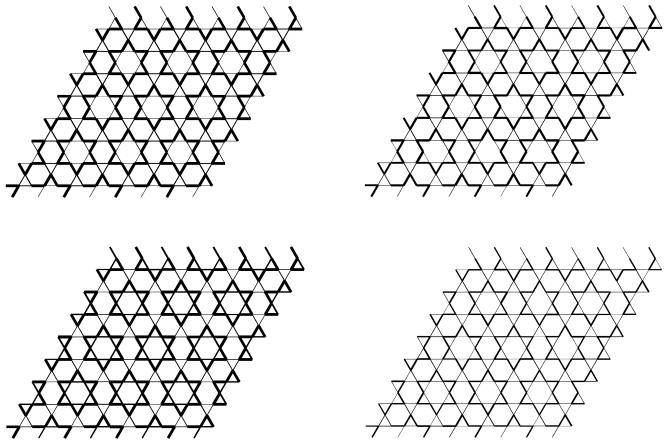

FIG. 8: Local bond measurements for $\alpha = 0.9$ and comparing two values of mu. Above: Spin-spin exchange. Below: kinetic energy. Left: $\mu = 0.0$ and Right: $\mu = 0.99$.

$t-J$ model.

This can be understood as in the Hubbard model the physics involved is more complex: In our wave-function we have two more free parameters compared to the $t-J$ model, which are the two projection operators. It is insightful to study the influence of them systematically: For this we keep one of the projectors constant and vary the other one. We observe the impact of them on the kinetic energy $\sum_{\langle ij\rangle}\langle c_i^\dagger c_j\rangle$, spin-spin exchange $\sum_{\langle ij\rangle}\langle S_iS_j\rangle$ and double-occupation $\langle d\rangle$. For this purpose we measure the involved observables not only in the bulk but also locally in terms of sites and bonds. We focus on the HVBC with $\chi \neq 1$. In Fig. 5 we fix μ and vary α. We consider first the case $\mu = 0$ and vary α: It is clear that spin-exchange $\langle S_iS_j\rangle$ will increase while the kinetic energy $c_i^\dagger c_j$ is decreasing with increasing α, as α controls the d. For $0 < \mu < 0.7$ we see that the combined effect is slightly more complicated as E_{KIN} develops a minimum at $\alpha = 0.05$ to $\alpha = 0.10$ depending on μ. Fixing α and varying μ we see two regimes which correspond to the phases below and above the Mott-transition (see Fig. 6). For $0 \leq \alpha \leq 0.6$ the measured d is rising, and therefore the spin-spin exchange decreases, while for $\alpha > 0.6$ there is the opposite trend.

More subtle is which type of pattern will emerge: We see that the increasing α leads to the type of pattern observed for the $t-J$ model at low doping: While the spin-exchange recovered the "input" of the HVBC (see Fig. 8), the kinetic energy develops a slightly derivation of this pattern, by weighting the inner hexagon stronger, than the connecting triangles. Now we set $\mu = 0.99$ and vary α: This case is more subtle as μ and α are influencing each other. We observe that the spin-exchange is

very weak for α low and increases with α while the kinetic energy has again the opposite trend. We note that the patterns emerging for the kinetic energy are similar to the ones of the $t-J$-model. Now we finally compare cases with finite α and its matching (in terms of optimized energy for a particular U) μ and compare this with the same α and $\mu = 0$: In this case $\mu = 0$ has a higher value for the spin-spin exchange but a lower value for the kinetic energy. This shows the subtlety of the combined effect.

To summarize we investigated the Hubbard model at half-filling and investigated the question whether the D-state can be stabilized in any regime for $U \neq \infty$. We study the trend of dimerization in that model, and find a qualitatively similar trend compared to the $t-J$ model. We can understand the differences when investigating the impact of the projection operators on the wave function. Further the interplay with the Mott-transition is an interesting aspect we found, possible relevant for a larger class of frustrated models. We have summed up the combined result of this paper and the two preceding ones on the $t-J$ model in Fig. 7, where we have indicated the point of optimal doping in the $t-J$ model, and the corresponding point of the similar value for the double occupation in the Hubbard model.

Acknowledgments: Supercomputer support was provided by the NIC, FZ Jülich under project No. HDO070 and by ITMC of TU-Dortmund.

[1] R. R. P. Singh and D. A. Huse, Phys. Rev. B **76**, 180407 (2007).
[2] Y. Iqbal, F. Becca, and D. Poilblanc, Phys. Rev. B, **84**, 020407(R) (2011).
[3] S. Yan, D. A. Huse, and S. R. White, Sience, **332** 1173 (2011).
[4] H. Nakano and T. Sakai, J. Phys. Soc. Jpn. **80** 05370, (2011).
[5] A. M. Laeuchli, J. Sudan, and E. S. Sorensen, Phys. Rev. B **83**, 212401 (2011).
[6] S. Depenbrock, I. P. McCulloch, and U. Schollwock, Phys. Rev. Lett., **109**, 067201 (2012).
[7] T. Imai, E. A. Nytko, B. M. Bartlett, M. P. Shores, and D. G. Nocera, Phys. Rev. Lett., **100**, 077203 (2008).
[8] A. Olariu, P. Mendels, F. Bert, F. Duc, J. C. Trombe, M. A. de Vries, and A. Harrison, Phys. Rev. Lett., **100**, 087202 (2008).
[9] M. P. Shores, E. A. Nytko, B. M. Bartlett, and D. G. Nocera, J. Am. Chem. Soc., **127**, 13462 (2005).
[10] P. Mendels, F. Bert, M. A. de Vries, A. Olariu, A. Harrison, F. Duc, J. C. Trombe, J. S. Lord, A. Amato, and C. Baines, Phys. Rev. Lett., **98**, 077204 (2007).
[11] M. A. de Vries, K. V. Kamenev, W. A. Kockelmann, J. Sanchez-Benitez, and A. Harrison, Phys. Rev. Lett., **100**, 157205 (2008).
[12] J. S. Helton, K. Matan, M. P. Shores, E. A. Nytko, B. M. Bartlett, Y. Yoshida, Y. Takano, A. Suslov, Y. Qiu, J.-H. Chung, D. G. Nocera, and Y. S. Lee, Phys. Rev. Lett., **98**, 107204 (2007).
[13] T. Ohashi, N. Kawakami, and H. Tsunetsugu, Phys. Rev. Lett., **97**, 066401 (2006).
[14] S. Kuratani, A. Koga, and N. Kawakami, J. Phys.: Condens. Matter, **19**, 145252, (2007).
[15] B. H. Bernhard, B. Canals, and C. Lacroix, J. Phys.: Condens. Matter, **19**, 145258, (2007).
[16] W. S. Wang, Z. Z. Li, Y. Y. Xiang, Q. H. Wang, Phys. Rev. B 87, 115135 (2013).
[17] M. L. Kiesel, C. Platt, R. Thomale, Phys. Rev. Lett. 110, 126405 (2013).
[18] S. Guertler and H. Monien, Phys. Rev. B, **84**, 174409 (2011).
[19] S. Guertler and H. Monien, Phys. Rev. Lett., **111**, 097204 (2013).
[20] M. B. Hastings, Phys. Rev. B, **63**, 014413 (2000).
[21] Y. Ran, M. Hermele, P. A. Lee, and X. G. Wen, Phys. Rev. Lett., **98**, 117205 (2007).
[22] Y. Iqbal, F. Becca, S. Sorella, and Didier Poilblanc, Phys. Rev. B, **87**, 060405 (2013).
[23] S. Guertler, Q. H. Wang, and F. C. Zhang, Phys. Rev. B, **79**, 144526 (2009).